Localized and distributed mass detectors with high sensitivity based on thin-film bulk acoustic resonators

Humberto Campanella, Jaume Esteve, Josep Montserrat, Arantxa Uranga, Gabriel Abadal, Nuria Barniol, and Albert Romano-Rodríguez

Citation: Applied Physics Letters **89**, 033507 (2006); doi: 10.1063/1.2234305
View online: http://dx.doi.org/10.1063/1.2234305
View Table of Contents: http://scitation.aip.org/content/aip/journal/apl/89/3?ver=pdfcov
Published by the AIP Publishing

Localized and distributed mass detectors with high sensitivity based on thin-film bulk acoustic resonators

Humberto Campanella,[a)] Jaume Esteve, and Josep Montserrat
Centro Nacional de Microelectrónica (CNM-IMB-CSIC), Microsystems and Nanotechnologies Group, Campus UAB, 08193 Bellaterra (Barcelona), Spain

Arantxa Uranga, Gabriel Abadal, and Nuria Barniol
Department of Electronics Engineering, School of Engineering, Universitat Autónoma de Barcelona, Edifici Q, 08193 Bellaterra (Barcelona), Spain

Albert Romano-Rodríguez
Department of Electronics, Universitat de Barcelona, c/Martí i Franquès 1, E-08028 Barcelona, Spain

(Received 3 February 2006; accepted 19 June 2006; published online 21 July 2006)

A mass sensor based on thin-film bulk acoustic resonator, intended for biomolecular applications, is presented. The thin film is a (002) AlN membrane, sputtered over Ti/Pt on a (001) Si wafer, and released by surface micromachining of silicon. Two experiments are proposed to test the mass sensing performance of the resonators: (a) distributed loading with a MgF_2 film by means of physical vapor deposition and (b) localized mass growing of a C/Pt/Ga composite using focused-ion-beam-assisted deposition, both on the top electrode. For the distributed and localized cases, the minimum detectable mass changes are 1.58×10^{-8} g/cm^2 and 7×10^{-15} g, respectively. © *2006 American Institute of Physics*. [DOI: 10.1063/1.2234305]

The interest for thin-film bulk acoustic resonators (FBARs) comprises several applications. In mass sensor applications, quartz crystal microbalances (QCMs) have been a key technology.[1] However, most recent and demanding applications—e.g., biomolecular or chemical detection—and the limited frequency range of QCM-based systems have created the need for conceiving devices with increased sensitivity. FBAR devices are able to replace QCM in such areas where higher mass sensitivity is required.[2–4] Other technological approaches, such as nanoelectromechanical system (NEMS) resonators, have also proved to achieve very high sensitivity in localized-mass detection applications.[5–7]

The FBAR-based mass sensor operates in the principle of mass loading, which is typically implemented by growing or depositing a thin film in one of the electrodes of the resonator. The fabrication technology determines the manner and the electrode in which the thin mass is deposited. The mass loading acts in the sensor's frequency response, by changing its resonance frequency $f_0=v_0/2t_0$, where v_0 and t_0 are sound velocity and thickness of the unloaded resonator, respectively. For added masses with density ρ_m and thickness $t_m \ll t_0$, the loaded resonance frequency f_m is evaluated in the Sauerbrey-Lostis equation[8–10] as

$$f_m = \frac{1}{f_0 + 2(\rho_m t_m/\rho_0 t_0)}. \quad (1)$$

In Eq. (1) the term at the right of f_0 corresponds to the frequency change Δf due to added mass Δm. In this way, the frequency change relative to the unloaded resonance frequency can be solved as

$$\frac{\Delta f}{f_0} \approx -\frac{\rho_m t_m}{\rho_0 t_0} = -\frac{\Delta m}{m_0}. \quad (2)$$

Equation (2) is valid if Δm is less than 2% of the initial mass of the resonator m_0. For the case of distributed mass sensors, two parameters are mainly considered to evaluate the performance: Mass sensitivity (cm^2/g), defined as $S_m = 1/\Sigma\rho_i t_i$, where ρ_i and t_i are density and thickness for each material layer in the resonator's stack, and frequency responsivity $R_f=\Delta f/f_0$, where Δf is the minimum detectable frequency shift.[11] The minimum detectable mass change per unit area can be evaluated from $\Delta m=R_f/S_m$. In the same way, mass responsivity per area r_m (g/Hz/cm^2) is calculated from $r_m=1/(f_0 S_m)$. On the other hand, for localized-mass deposition, mass responsivity R_m is the change in frequency response per unit mass change (Hz/g), but in certain cases it is more convenient to deal with the inverse responsivity (g/Hz). In this letter, the word *responsivity* will be used to express *inverse responsivity*, being the minimum detectable mass change calculated as the product $\Delta f R_m$.[12] A typical value for a QCM operating at 40 MHz can be found in the units of ng/Hz/cm^2, while for a FBAR operating at 1 GHz this value reaches the units of pg/Hz/cm^2, i.e., 1000 better for the latter.[13,14] In this work, focus is laid on the exploration of different capabilities of FBAR as mass sensors as it is the case of localized-mass detection.

The FBAR was implemented as a sandwiched (002) aluminum nitride (AlN) membrane (1 μm thick), sputtered on top of a titanium/platinum (Ti/Pt) layer (30/150 nm thick) deposited on a (001) silicon (Si) substrate, and released by surface micromachining of the silicon substrate (Fig. 1). Two

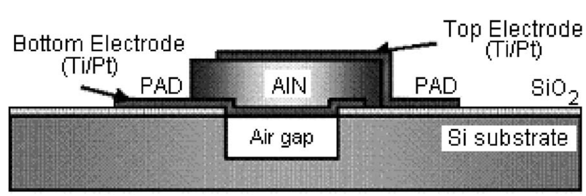

FIG. 1. Side view of the FBAR process.

[a)]Electronic mail: hcampane@cnm.es

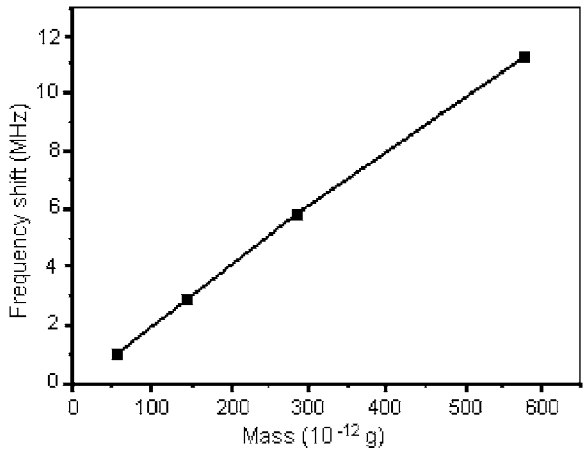

FIG. 2. Frequency shifting vs mass loading (uniform-mass case): a linear behavior is observed for irregular rhomboid devices.

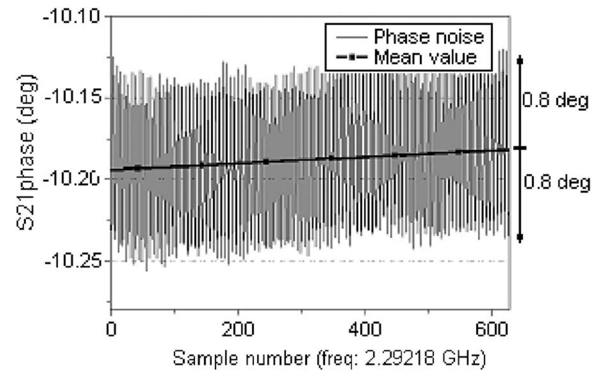

FIG. 3. Zero-span plot of the S21 phase response (deg) of a FBAR. Phase noise is evaluated as the maximum deviation from the mean phase value (0.8 deg). This value is divided by the slope at the resonance frequency (2.65×10^{-6} deg/Hz at 2.29 GHz) to calculate the minimum detectable phase frequency shift, which is employed in evaluating the minimum detectable mass.

different geometries and sizes for the FBAR electrodes were designed, being one of them a rectangular-shaped device (50×70 μm^2), and the second one an irregular rhomboid (70×130 μm^2). For this configuration, the FBAR resonates in the 2 GHz range, and its theoretical mass responsivity per area is 4.15×10^{-13} g/Hz/cm^2.

Concerning the experiments to deposit mass on the FBAR, the whole surface of the top electrode of several devices was covered with a physical-vapor-deposited uniform thin film of magnesium fluoride (MgF_2), with different thicknesses—2, 5, 10, and 20 nm—in diverse samples. Taking into consideration these thicknesses, four groups of resonators were characterized. As expected, the resonance frequency shifted down several megahertz, in linear proportion to the amount of deposited mass (Fig. 2).

As a general comment, this experiment does not exceed the limits for the Sauerbrey-Lostis equation to be valid, being the ratio $\Delta m/m_0$ between 0.06% and 0.64%. Hence, from the frequency shifting and deposited mass data in Fig. 2, the experimental *mass responsivity per area* was found to be 5.23×10^{-13} g/Hz/cm^2, which is 80% of the theoretical value for the current FBAR stack configuration. The *minimum mass change* that can be detected with the current measurement setup and FBAR configuration is evaluated by checking the minimum detectable frequency shift, which occurred to be $\Delta f=30$ kHz, thus obtaining a value of 1.58×10^{-8} g/cm^2. The minimum frequency shifting was found from the phase of the S21 parameter. First, the phase noise is quantified from a zero-span acquisition observing the series resonance frequency (Fig. 3). As observed in Fig. 3, the maximum deviation from the mean phase value is 0.8 deg, which is divided by the phase slope—2.65×10^{-6} deg/Hz. This value is calculated from differentiation of the S21 phase and evaluated at the series resonance frequency.

In a second experiment, deposition in selected areas of a second set of resonators has been performed inside a focused-ion-beam (FIB) machine, in order to test their capabilities for localized-mass detection. For this, a platinum-containing metal organic precursor, injected in the sample's chamber, has been decomposed by the ion beam, giving rise to the localized deposition of an amorphous compound that contains C, Pt, and Ga (65%, 27%, and 8%, respectively) in the area scanned by the beam,[15] whose mass density being around 4 g/cm^3. In these experiments different-sized square depositions have been tested. By localized-mass deposition we must understand the deposition of a material, whose contact surface with the resonator is quite small, compared with the effective resonator's surface. In fact, the deposited mass area for each one of the samples is always less than 0.7% of the electrode surface. The scanning electron microscope (SEM) image of Fig. 4(a) shows a rectangular-surface mass, deposited on the center of the top Ti/Pt electrode of a rectangular FBAR, with an enlarged view in Fig. 4(b).

As in the uniform-mass case, a direct proportionality in the frequency and mass changes is observed for the localized-mass deposition (Fig. 5). For this latter case, downshifting of resonance frequency is higher, even for smaller deposited masses. This situation suggests an increase on the mass responsivity for FBAR sensors in localized-mass applications.

Additional information concerning the mass loading are obtained in Table I, where responsivities and minimum mass detectable are compared for the cases of distributed and localized loadings, showing that the localized-loading case has figures of performance that are one order of magnitude higher. For example, the mass responsivity R_m of the FBAR—an average of 2.38×10^{-19} g/Hz—is better, compared with those of mass sensors based on NEMS resonators.[5,6] Concerning the calculation of mass sensitivity, it is deduced from the product $\Delta f R_m$, obtaining a value of 7.18×10^{-15} g. Further experiments would allow the extrac-

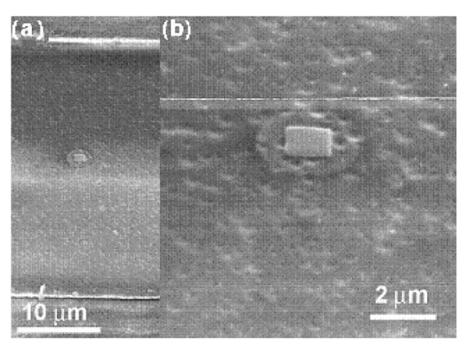

FIG. 4. (a) SEM image of a localized mass deposited on a rectangular FBAR sensor (the upper and lower edges of the FBAR are the horizontal bright lines in the image) and (b) larger magnification. A halo is observed around the mass which is caused by slight contamination during the deposition process. The images are taken tilted 52° around a horizontal axis.

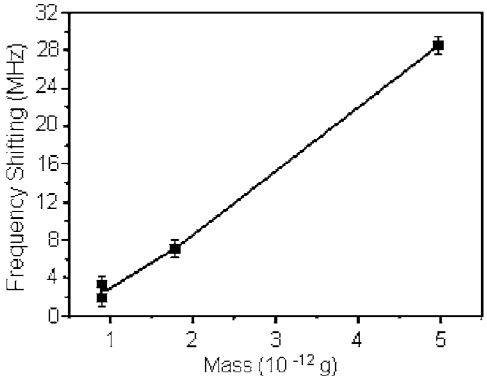

FIG. 5. Frequency shifting vs mass loading (localized-mass case) for the second group of FBAR illustrates the proportional change in frequency with loaded mass. Masses are square area shaped of a C/Pt/Ga composite deposited on different FBARs. The upper right point corresponds to a mass of 4.97×10^{-12} g with surface of 25 μm^2, deposited on a first FBAR. The remaining points correspond to masses deposited on other resonators, each mass with a deposited area of 2.25 μm^2. Frequency dispersion is accounted for the current setup resolution.

tion of the ultimate sensitivity of FBAR operating at 2 GHz. In fact, a refinement of the setup should leverage the minimum frequency shift to values as low as units of hertz, thus increasing the sensitivity to the range of attograms. Several measures such as probe table shielding or vacuum chamber adaptation should be implemented, in order to investigate noise sources and the strategies to overcome them.

TABLE I. Mass responsivities and minimum detectable mass for distributed and localized-mass depositions. Presented values are averaged for a set of resonators and evidence performance figures that are one order of magnitude higher for the localized-mass case. For the localized-mass case, responsivity and minimum detectable mass are not evaluated by unit area, since deposition and FBAR surface areas are not comparable.

Case	Mass responsivity R_m (g/Hz)	Mass responsivity per area r_m (g/Hz/cm^2)	Minimum detectable mass (g)	Minimum detectable mass per area (g/cm^2)
Localized-mass loading	2.38×10^{-19}	⋯	7.18×10^{-15}	⋯
Distributed-mass loading	4.71×10^{-17}	5.23×10^{-13}	1.42×10^{-12}	1.58×10^{-8}

From the presented results, piezoelectric-based thin-film sensors appear as a candidate technology alternative to NEMS for very high mass sensitive applications. It has been experienced that, as only a very small fraction of the overall electrode area is loaded, the responsivity is increased between one and two orders of magnitude, compared with the uniform-deposition case. This discovery could be used to detect localized particles and allows the application of FBAR as biological mass sensor where selective spatial detection is required.

In these initial experiments, the ability of FBAR as high-responsivity, high-sensitivity localized-mass sensors has been demonstrated. Further study would allow to understand the eventual relationship between the location in which localized mass is deposited and the resonance modes of the sensor. Also, the development of improved setups for measuring the mass sensitivity is needed to evaluate the possibilities and target applications of FBAR-based mass detection.

[1] C. S. Lu, *Applications of Piezoelectric Quartz Crystal Microbalance* (Elsevier, London, 1984).
[2] M. Benetti, D. Cannatà, F. Di Pietrantonio, V. Foglietti, and E. Verona, Appl. Phys. Lett. **87**, 173504 (2005).
[3] M. Benetti, D. Cannatà, A. D'Amico, F. Di Pietrantonio, V. Foglietti, and E. Verona, Proc.-IEEE Ultrason. Symp. **3**, 1581 (2004).
[4] H. Zhang and E. S. Kim, J. Microelectromech. Syst. **14**, 699 (2005).
[5] E. Forsen, G. Abadal, S. Ghatnekar-Nilsson, J. Teva, J. Verd, R. Sandberg, W. Svendsen, F. Perez-Murano, J. Esteve, E. Figueras, F. Campabadal, L. Montelius, N. Barniol, and A. Boisen, Appl. Phys. Lett. **87**, 043507 (2005).
[6] K. L. Ekinci, X. M. H. Huang, and M. L. Roukes, Appl. Phys. Lett. **84**, 4469 (2004).
[7] B. Ilic, H. G. Craighead, S. Krylov, W. Senaratne, C. Ober, and P. Neuzil, J. Appl. Phys. **95**, 3694 (2004).
[8] G. Z. Sauerbrey, Phys. Verh. **8**, 193 (1957).
[9] G. Z. Sauerbrey, Z. Phys. **155**, 206 (1959).
[10] P. Lostis, Rev. Opt., Theor. Instrum. **38**, 1 (1959).
[11] S. W. Wenzel and R. M. White, Appl. Phys. Lett. **54**, 1976 (1989).
[12] K. L. Ekinci, Y. T. Yang, and M. L. Roukes, J. Appl. Phys. **95**, 2682 (2004).
[13] R. Gabl, H.-D. Feucht, H. Zeininger, G. Eckstein, M. Schreiter, R. Primig, D. Pitzer, and W. Wersing, Biosens. Bioelectron. **19**, 615 (2004).
[14] H. Zhang, M. S. Marma, E. S. Kim, C. E. McKenna, and M. E. Thompson, J. Micromech. Microeng. **15**, 1911 (2005).
[15] A. Vilà, F. Hernández-Ramírez, J. Rodríguez, O. Casals, A. Romano-Rodríguez, J. R. Morante, and M. Abid, Mater. Sci. Eng., C **26**, 1063 (2006).